

Physical implementation for entanglement purification of Gaussian continuous variable quantum states

Lu-Ming Duan^{1,2*}, G. Giedke¹, J. I. Cirac¹, and P. Zoller¹

¹*Institut für Theoretische Physik, Universität Innsbruck, A-6020 Innsbruck, Austria*

²*Department of Physics, University of Science and Technology of China, Hefei 230026, China*

We give a detailed description of the entanglement purification protocol which generates maximally entangled states with high efficiencies from realistic Gaussian continuous variable entangled states. The physical implementation of this protocol is extensively analyzed using high finesse cavities and cavity enhanced cross Kerr nonlinearities. In particular, we take into account many imperfections in the experimental scheme and calculate their influences. Quantitative requirements are given for the relevant experimental parameters.

PACS numbers: 03.67.Hk, 42.50.-p, 03.65.Bz

I. INTRODUCTION

Quantum entanglement plays an essential role in many interesting quantum information protocols, such as in quantum key distribution and quantum teleportation [1]. To faithfully realize these protocols, first we need to generate a maximally entangled state. In reality, however, due to loss and decoherence, normally we can only generate partially entangled states between distant sides [2]. Entanglement purification is further needed which distills a maximally entangled state from several pairs of partially entangled states using local quantum operations and classical communications [3,4]. For qubit systems, efficient entanglement purification protocols have been found [4,5]. Recently, quantum information protocols have been extended from qubit systems to continuous variable systems, such as continuous variable teleportation [6,7], continuous variable computation [8] and error correction [9], continuous variable cryptography [10], and also the notions of continuous variable inseparability [11] and bound entanglement [12] have been investigated. For physical implementation, Gaussian continuous variable entangled states (i.e., states whose Wigner functions are Gaussians) can be generated experimentally by transmitting two-mode squeezed light, and this kind of entanglement has been demonstrated in the recent experiment of continuous variable teleportation [13]. Obviously, it is useful to consider purification of continuous variable entanglement, that is, to generate a desired more entangled state from some realistic continuous entangled states. We have recently proposed an efficient continuous variable entanglement purification protocol [14]. In this paper, we present the mathematical details of this purification

protocol together with new results on its physical implementation. In particular, we take into account many important imperfections in a realistic experimental setup, and calculate their influence on the purification scheme. Quantitative requirements are given for the relevant experimental parameters. These calculations make necessary preparations for a real experiment. We also show how to generate Gaussian continuous entangled states between two distant high finesse cavities, which is the first step for the physical implementation of the purification protocol.

It should be noted that with direct extensions of the purification protocols for qubit systems, it is possible to increase entanglement for a special class of less realistic continuous entangled states [15]. Unfortunately, with these direct extensions no entanglement increase has been found till now for realistic Gaussian continuous entangled states. In [16] a protocol to increase the entanglement for the special case of pure two-mode squeezed states has been proposed, which is based on conditional photon subtraction. For its practical realization, the efficiency, however, seems to be an issue. In contrast, the purification scheme discussed in this paper has the following favorable properties: (i) For pure states it reaches the maximal allowed efficiency in the asymptotic limit (when the number of pairs of modes goes to infinity); (ii) It can be readily extended to distill maximally entangled states from a relevant class of mixed Gaussian states which result from losses in the light transmission; (iii) An experimental scheme is possible for physical implementation of the purification protocol using high finesse cavities and cross Kerr nonlinearities.

The paper is arranged as follows: In section 2 we show how to generate a Gaussian continuous entangled state between two distant cavities from the broadband squeezed light provided by a nondegenerate optical parametric amplifier (NOPA). Light transmission loss is taken into account. In sections 3 and 4 we give a detailed description of the purification protocol. Section 3 shows how to generate a maximally entangled state from pure two-mode squeezed states based on a local quantum nondemolition (QND) measurement of the total photon number, and section 4 extends the purification protocol to include the mixed Gaussian continuous states which are evolved from the pure two-mode squeezed states due to the unavoidable light transmission loss. In section 5, we describe a cavity scheme to realize the local QND measurement of the total photon number, and deduce conditions for the QND measurement. Then, in section 6, we

*Email: luming.duan@uibk.ac.at

extensively discuss many imperfections for a real experiment on QND measurements, and deduce quantitative requirements for the relevant experimental parameters. Last, we summarize the results, and give some typical parameter estimations.

II. GENERATION OF CONTINUOUS ENTANGLED STATES BETWEEN TWO DISTANT CAVITIES

Our source of entangled light field is taken to be a NOPA operating below threshold [17]. The light fields may be nondegenerate in polarization or in frequency. The two NOPA cavity modes c_A and c_B are assumed to have the same output coupling rate κ_c . The dynamic in the NOPA cavity is described by the Langevin equations (in the rotating frame) [18]

$$\begin{aligned}\dot{c}_A &= \epsilon c_B^\dagger - \frac{\kappa_c}{2} c_A - \sqrt{\kappa_c} c_{iA}, \\ \dot{c}_B^\dagger &= \epsilon^* c_A - \frac{\kappa_c}{2} c_B^\dagger - \sqrt{\kappa_c} c_{iB}^\dagger,\end{aligned}\quad (1)$$

where ϵ is the pumping rate with $|\epsilon| < \kappa_c/2$ (below threshold), and c_{iA} and c_{iB} are vacuum inputs. The NOPA outputs c_{oA} and c_{oB} are given respectively by $c_{o\alpha} = c_{i\alpha} + \sqrt{\kappa_c} c_\alpha$ ($\alpha = A, B$). The two outputs, perhaps after a long distance propagation, are incident on distant high finesse cavities A and B. The cavities A and B are assumed to have the same damping rate κ with $\kappa \ll \kappa_c$. The schematic setup is shown by Fig. 1.

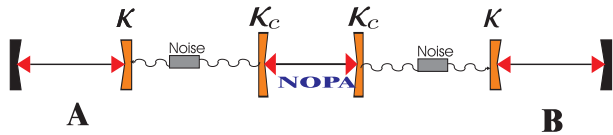


FIG. 1. Schematic setup for generating Gaussian continuous entangled states between two distant cavities.

Under the condition $\kappa \ll \kappa_c$, the dynamics in the NOPA cavity is much faster than those in the cavities A and B, so we can assume a steady state for the NOPA outputs. The steady NOPA outputs are described by squeezed white noise operators with the following correlations [18]

$$\begin{aligned}\langle c_{oA}(t) c_{oB}(t') \rangle &= M \delta(t - t'), \\ \langle c_{o\alpha}^\dagger(t) c_{o\alpha}(t') \rangle &= N \delta(t - t'), \quad (\alpha = A, B), \\ \langle c_{o\alpha}(t) c_{o\alpha}^\dagger(t') \rangle &= (N + 1) \delta(t - t'), \quad (\alpha = A, B),\end{aligned}\quad (2)$$

where N and M , satisfying $M = \sqrt{N(N+1)}$, are determined by the NOPA coupling and pumping rates through $N = |\epsilon|^2 \kappa_c^2 / \left(\frac{\kappa_c^2}{4} - |\epsilon|^2\right)^2$ and $M = |\epsilon| \kappa_c \left(\frac{\kappa_c^2}{4} + |\epsilon|^2\right) / \left(\frac{\kappa_c^2}{4} - |\epsilon|^2\right)^2$.

To get the steady state of the cavities A and B, we note that their inputs a_{iA} and a_{iB} are respectively the

NOPA outputs c_{oA} and c_{oB} with neglect of the losses during light propagation. The Langevin equations for the cavity modes a_A and a_B have the form

$$\dot{a}_\alpha = -\frac{\kappa}{2} a_\alpha - \sqrt{\kappa} a_{i\alpha}, \quad (\alpha = A, B),$$

with the following solution

$$a_\alpha(t) = a_\alpha(0) e^{-\frac{\kappa}{2}t} - \sqrt{\kappa} \int_0^t e^{-\frac{\kappa}{2}(t-t')} a_{i\alpha}(t') dt'. \quad (3)$$

When κt is considerably larger than 1, from Eqs. (2) and (3), it follows that

$$\begin{aligned}\langle a_A a_B \rangle &= \sqrt{N(N+1)}, \\ \langle a_\alpha^\dagger a_\alpha \rangle &= N, \quad (\alpha = A, B), \\ \langle a_\alpha a_\alpha^\dagger \rangle &= (N+1), \quad (\alpha = A, B).\end{aligned}\quad (4)$$

On the other hand, we know that two modes driven by a white noise are in Gaussian states at any time. A Gaussian state with the correlations (4) is necessarily a pure two-mode squeezed state. So the steady state of the cavity modes a_A and a_B is

$$|\Psi\rangle_{12} = S_{AB}(r) |\text{vac}\rangle_{AB}, \quad (5)$$

where the squeezing operator $S_{AB}(r) = \exp\left[r\left(a_A^\dagger a_B^\dagger - a_A a_B\right)\right]$ and the squeezing parameter r is determined by $\coth(r) = \sqrt{N+1}$.

Next we include some important sources of noise in the state generation process. The noise includes the losses in the NOPA cavity and the light transmission loss from the NOPA cavity to the cavities A and B. With a small loss rate $\eta_0 \ll \kappa_c$ for the modes c_A and c_B in the NOPA cavity, the Langevin equation (1) is replaced by

$$\begin{aligned}\dot{c}_A &= \epsilon c_B^\dagger - \frac{\kappa_c + \eta_0}{2} c_A - \sqrt{\kappa_c} c_{iA} - \sqrt{\eta_0} v_{iA}, \\ \dot{c}_B^\dagger &= \epsilon^* c_A - \frac{\kappa_c + \eta_0}{2} c_B^\dagger - \sqrt{\kappa_c} c_{iB}^\dagger - \sqrt{\eta_0} v_{iB}^\dagger,\end{aligned}\quad (6)$$

where v_{iA} and v_{iB} are standard vacuum white noise, and the NOPA outputs are still given by $c_{o\alpha} = c_{i\alpha} + \sqrt{\kappa_c} c_\alpha$ ($\alpha = A, B$). On the other hand, the transmission loss of light can be described by

$$a_{i\alpha} = c_{o\alpha} \sqrt{e^{-\eta_\alpha \tau}} + v_\alpha \sqrt{1 - e^{-\eta_\alpha \tau}}, \quad (\alpha = A, B), \quad (7)$$

where τ is the transmission time, η_A and η_B are respectively the transmission loss rates for the outputs c_{oA} and c_{oB} , and v_A and v_B are standard vacuum white noise. From Eqs. (6) and (7), it follows that the inputs for the cavities A and B have the following correlations

$$\begin{aligned}\langle a_{iA}(t) a_{iB}(t') \rangle &= \sqrt{N'(N'+1)} e^{-\frac{\eta'_A + \eta'_B}{2} \tau} \delta(t - t'), \\ \langle a_{i\alpha}^\dagger(t) a_{i\alpha}(t') \rangle &= N' e^{-\eta'_\alpha \tau} \delta(t - t'), \quad (\alpha = A, B), \\ \langle a_{i\alpha}(t) a_{i\alpha}^\dagger(t') \rangle &= \left(N' e^{-\eta'_\alpha \tau} + 1\right) \delta(t - t'), \quad (\alpha = A, B).\end{aligned}$$

where the total loss rates $\eta'_\alpha = \eta_\alpha + \frac{1}{\tau} \ln(1 + \eta_0/\kappa_c) = \eta_\alpha + \eta_0/(\kappa_c\tau)$ ($\alpha = A, B$), and the parameter $N' = |\epsilon|^2 (\kappa_c + \eta_0)^2 / \left(\frac{(\kappa_c + \eta_0)^2}{4} - |\epsilon|^2 \right)^2 \approx N$. The steady state of the two cavity modes a_A and a_B is thus a Gaussian state with the non-zero correlations given by

$$\begin{aligned} \langle a_A a_B \rangle &= \sqrt{N(N+1)} e^{-\frac{\eta'_A + \eta'_B}{2} \tau}, \\ \langle a_\alpha^\dagger a_\alpha \rangle &= N e^{-\eta'_\alpha \tau}, \quad (\alpha = A, B), \\ \langle a_\alpha a_\alpha^\dagger \rangle &= \left(N e^{-\eta'_\alpha \tau} + 1 \right), \quad (\alpha = A, B). \end{aligned} \quad (8)$$

The Gaussian state is completely determined by these correlations. The Gaussian state (8) can be equivalently described as the solution at time $t = \tau$ of the following master equation

$$\begin{aligned} \dot{\rho} &= \eta'_A \left(a_A \rho a_A^\dagger - \frac{1}{2} a_A^\dagger a_{A1} \rho - \frac{1}{2} \rho a_A^\dagger a_A \right) \\ &\quad + \eta'_B \left(a_B \rho a_B^\dagger - \frac{1}{2} a_B^\dagger a_{B1} \rho - \frac{1}{2} \rho a_B^\dagger a_B \right) \end{aligned} \quad (9)$$

with the initial state $\rho(0) = |\Psi\rangle_{AB} \langle \Psi|$, where $|\Psi\rangle_{AB}$ is defined by Eq. (5). This equivalence simplifies the physical picture in section 4, where we will use the master equation (9) to describe the state generation noise.

III. ENTANGLEMENT CONCENTRATION OF PURE TWO-MODE SQUEEZED STATES

In the above, we have shown how to generate continuous partially entangled states between two distant cavities. In the case of no noise in the state generation process, the cavities are in a pure two-mode squeezed state. In this section, we will show how to concentrate continuous variable entanglement, that is, starting from several pairs of continuous entangled states, we want to get a state with more entanglement through only local operations. The section is divided into two parts. The first part describes the purification protocol for two entangled pairs, and the second part extends the protocol to include multiple pairs.

A. Concentration of two entangled pairs

Assume now we have two cavities A_1, A_2 and B_1, B_2 on each side. Each pair of cavities A_i, B_i ($i = 1, 2$) are prepared in the state (5), which is now denoted by $|\Psi\rangle_{A_i B_i}$. $|\Psi\rangle_{A_i B_i}$, expressed in the number basis, has the form

$$|\Psi\rangle_{A_i B_i} = \sqrt{1 - \lambda^2} \sum_{n=0}^{\infty} \lambda^n |n\rangle_{A_i} |n\rangle_{B_i}, \quad (10)$$

where $\lambda = \tanh(r)$. Equation (10) is just the Schmidt decomposition of the state $|\Psi\rangle_{A_i B_i}$. For a pure state,

the entanglement is uniquely quantified by the von Neumann entropy of the reduced density operator of its one-component. The entanglement of the state (10) is thus expressed as

$$E(|\Psi\rangle_{A_i B_i}) = \cosh^2 r \log(\cosh^2 r) - \sinh^2 r \log(\sinh^2 r). \quad (11)$$

The joint state of the two entangled pairs A_1, B_1 and A_2, B_2 is simply the product

$$\begin{aligned} |\Psi\rangle_{A_1 B_1 A_2 B_2} &= S_{A_1 B_1}(r) |\text{vac}\rangle_{A_1 B_1} \otimes S_{A_2 B_2}(r) |\text{vac}\rangle_{A_2 B_2} \\ &= (1 - \lambda^2) \sum_{j=0}^{\infty} \lambda^j \sqrt{1 + j} |j\rangle_{A_1 A_2 B_1 B_2}, \end{aligned} \quad (12)$$

where $|j\rangle_{A_1 A_2 B_1 B_2}$ is defined as

$$|j\rangle_{A_1 A_2 B_1 B_2} = \frac{1}{\sqrt{1 + j}} \sum_{n=0}^j |n, j - n\rangle_{A_1 A_2} |n, j - n\rangle_{B_1 B_2}. \quad (13)$$

We now perform a local QND measurement of the total photon number of the two cavities A_1, A_2 . There have been several proposals for doing QND measurements of the photon number, and in section 5, we will describe a cavity scheme for realizing the QND measurement of the total photon number of two local cavities. Here we simply assume this type of measurement can be done. After the QND measurement of the total number $n_{A_1} + n_{A_2}$, the state $|\Psi\rangle_{A_1 B_1 A_2 B_2}$ is collapsed into $|j\rangle_{A_1 A_2 B_1 B_2}$ with probability

$$p_j = (1 - \lambda^2)^2 \lambda^{2j} (j + 1). \quad (14)$$

The state $|j\rangle_{A_1 A_2 B_1 B_2}$ is a maximally entangled state between the two parties A_1, A_2 and B_1, B_2 in a $(j + 1) \times (j + 1)$ -dimensional Hilbert space, and its entanglement is

$$E(|j\rangle_{A_1 A_2 B_1 B_2}) = \log(j + 1). \quad (15)$$

If $E(|j\rangle_{A_1 A_2 B_1 B_2}) > E(|\Psi\rangle_{A_i B_i})$, i.e. $j > \frac{(\cosh(r))^{\cosh(r)}}{(\sinh(r))^{\sinh(r)}} - 1$, we get a two-party state with more entanglement. The quantity $\Gamma_j = \frac{E(|j\rangle_{A_1 A_2 B_1 B_2})}{E(|\Psi\rangle_{A_i B_i})}$ defines the entanglement increase ratio. Fig. 2 shows the probability of success versus entanglement increase ratio for some typical values of the squeezing parameter.

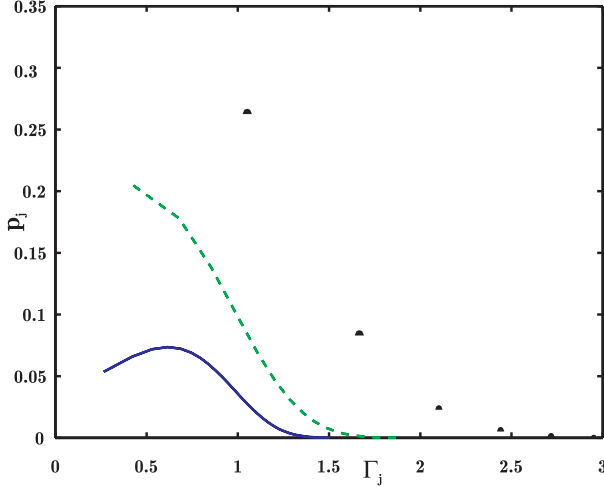


FIG. 2. The purification success probability versus entanglement increase ratio for two pairs. Dotted line for the squeezing parameter $r = 0.5$, dashed line for $r = 1.0$, and solid line for $r = 1.5$.

An interesting feature of this entanglement purification protocol is that with any measurement outcome $j \neq 0$, we always get a useful maximally entangled state in some finite Hilbert space, though the entanglement of the outcome state $|j\rangle_{A_1 A_2 B_1 B_2}$ does not necessarily exceed that of the original state $|\Psi\rangle_{A_i B_i}$ if j is small. The state $|j\rangle_{A_1 A_2 B_1 B_2}$ involves two pairs of cavities. If one wants to transfer the entanglement to a single pair of cavity modes, one can make a phase measurement of the cavity mode A_2 . There have been some proposals for doing a phase measurement [19,20]. A phase measurement of the mode A_2 with the measurement outcome ϕ will convert the state $|j\rangle_{A_1 A_2 B_1 B_2}$ to the following maximally entangled state of a single pair of cavity modes

$$|j\rangle_{A_1 A_2} = \frac{1}{\sqrt{1+j}} \sum_{n=0}^j e^{i(j-n)\phi} |n\rangle_{A_1} |n\rangle_{B_1}. \quad (16)$$

B. Concentration of multiple entangled pairs

The above protocol can be extended straightforwardly to simultaneously concentrate entanglement of multiple cavity-pairs. Simultaneous concentration of multiple entangled pairs is much more effective than the entanglement concentration two by two. Assume that we have m cavity-pairs $A_1, B_1, A_2, B_2, \dots$ and A_m, B_m . Each pair of cavities A_i, B_i is prepared in the state (10). The joint state of the m entangled pairs can be expressed as

$$\begin{aligned} |\Psi\rangle_{(A_i B_i)} &= |\Psi\rangle_{A_1 B_1} \otimes |\Psi\rangle_{A_2 B_2} \otimes \dots \otimes |\Psi\rangle_{A_m B_m} \\ &= (1 - \lambda^2)^{\frac{m}{2}} \sum_{j=0}^{\infty} \lambda^j \sqrt{f_j^{(m)}} |j\rangle_{(A_i B_i)}, \end{aligned} \quad (17)$$

where $(A_i B_i)$ is abbreviation of $A_1, B_1, A_2, B_2, \dots, A_m, B_m$, and the normalized state $|j\rangle_{(A_i B_i)}$ is defined as

$$|j\rangle_{(A_i B_i)} = \frac{1}{\sqrt{f_j^{(m)}}} \sum_{\substack{i_1, i_2, \dots, i_m \\ i_1 + i_2 + \dots + i_m = j}} |i_1, i_2, \dots, i_m\rangle_{(A_i)} \otimes |i_1, i_2, \dots, i_m\rangle_{(B_i)} \quad (18)$$

The function $f_j^{(m)}$ in Eqs. (17) and (18) is given by

$$f_j^{(m)} = \frac{(j+m-1)!}{j!(m-1)!} = \binom{j+m-1}{m-1}. \quad (19)$$

To concentrate the entanglement, we perform a QND measurement of the total photon number $n_{A_1} + n_{A_2} + \dots + n_{A_m}$. This measurement projects the state $|\Psi\rangle_{(A_i B_i)}$ onto a two-party maximally entangled state $|j\rangle_{(A_i B_i)}$ with probability

$$p_j^{(m)} = (1 - \lambda^2)^m \lambda^{2j} f_j^{(m)}. \quad (20)$$

The entanglement of the outcome state $|j\rangle_{(A_i B_i)}$ is given by

$$E(|j\rangle_{(A_i B_i)}) = \log(f_j^{(m)}). \quad (21)$$

Similarly, $\Gamma_j = E(|j\rangle_{(A_i B_i)}) / E(|\Psi\rangle_{A_i B_i})$ defines the entanglement increase ratio, and if $\Gamma_j > 1$, we get a more entangled state. For four pairs, the probability of success versus entanglement increase ratio is shown in Fig. 3. There appears a peak in the probability curve for some entanglement increase ratio between 2 and 3.

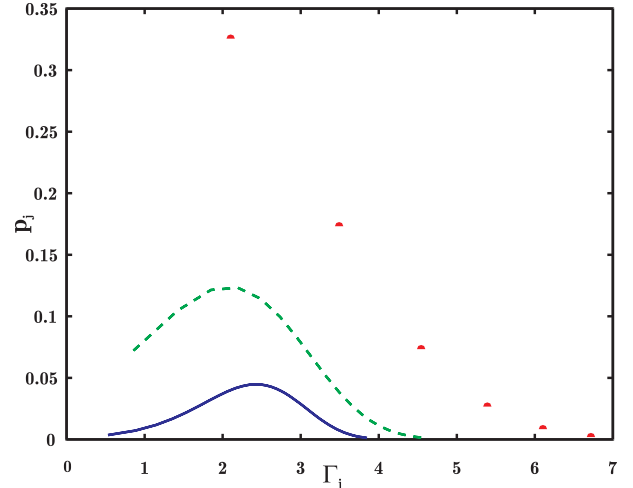


FIG. 3. The purification success probability versus entanglement increase ratio for the number of pairs $m = 4$. Dotted line for the squeezing parameter $r = 0.5$, dashed line for $r = 1.0$, and solid line for $r = 1.5$.

To measure how efficient the scheme is, we define the entanglement transfer efficiency Υ with the expression

$$\Upsilon = \frac{\sum_{j=0}^{\infty} p_j^{(m)} E(|j\rangle_{(A_i B_i)})}{mE(|\Psi\rangle_{A_i B_i})}. \quad (22)$$

It is the ratio of the average entanglement after concentration measurement to the initial total entanglement contained in the m pairs. Obviously, $\Upsilon \leq 1$ should always hold. With the squeezing parameter $r = 0.5, 1.0$ or 1.5 , the entanglement transfer efficiency versus the number of pairs m is shown in Fig. 4.

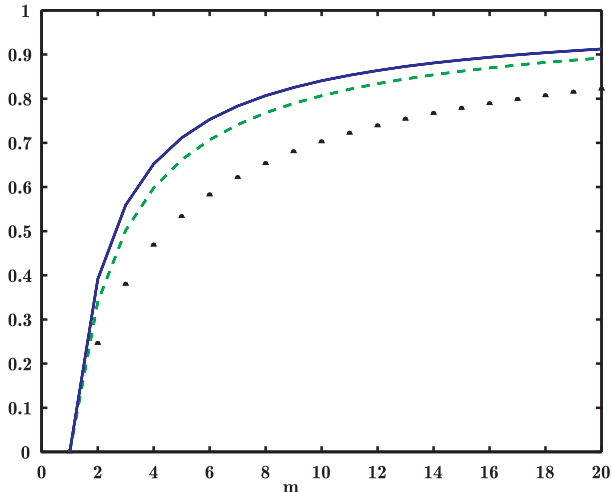


FIG. 4. The entanglement transfer efficiency versus the number of pairs m in simultaneous concentration. Dotted line for $r = 0.5$, dashed line for $r = 1.0$, and solid line for $r = 1.5$.

From the figure, we see that the entanglement transfer efficiency is near to 1 for a large number of pairs. In fact, it can be proven that if m goes to infinity, with unit probability we would get a maximally entangled state with entanglement $mE(|\Psi\rangle_{A_i B_i})$. To show this, we calculate the mean value and the variance of the distribution $p_j^{(m)}$, and find

$$\begin{aligned} \bar{j} &= \frac{m\lambda^2}{(1-\lambda^2)}, \\ \overline{(\Delta j)^2} &= \frac{m\lambda^2}{(1-\lambda^2)^2}. \end{aligned} \quad (23)$$

The results show that if m tends to infinity, $\sqrt{\overline{(\Delta j)^2}}/\bar{j} \rightarrow 0$ and the distribution $p_j^{(m)}$ tends to a δ -like function. Furthermore, around the mean value \bar{j} , the entanglement of the resulting state $|\bar{j}\rangle_{(A_i B_i)}$ is

$$E(|\bar{j}\rangle_{(A_i B_i)}) \xrightarrow{m \rightarrow \infty} mE(|\Psi\rangle_{A_i B_i}), \quad (24)$$

so the entanglement transfer efficiency tends to unity. This proves that the purification method described above

is optimal in the asymptotic limit ($m \rightarrow \infty$), analogous to the purification presented in [4] for the qubit case. For any finite number of entangled pairs, this purification protocol is more efficient than that in [4], since it takes advantage of the special relations between the coefficients in the two-mode squeezed state.

IV. ENTANGLEMENT PURIFICATION OF MIXED GAUSSIAN CONTINUOUS ENTANGLED STATES

The assumption of noise-free preparation of partially continuous entangled states is not realistic. If we include the unavoidable light transmission loss and the NOPA cavity loss in the state generation process, in section 2 we have shown that we would get a mixed Gaussian continuous entangled state between two distant cavities. The state is described by the solution at the transmission time τ of the master equation (9), with the ideal two-mode squeezed state (10) at the beginning. If we want to establish m entangled cavity-pairs $A_1, B_1, A_2, B_2, \dots$ and A_m, B_m , Eq. (9) can be extended directly to the following form

$$\dot{\rho} = -i(H_{\text{eff}}\rho - \rho H_{\text{eff}}^\dagger) + \sum_{i=1}^m \left(\eta'_A a_{A_i} \rho a_{A_i}^\dagger + \eta'_B a_{B_i} \rho a_{B_i}^\dagger \right) \quad (25)$$

where ρ is the density operator of the whole m entangled pairs with $\rho(0) = |\Psi\rangle_{(A_i B_i)}\langle\Psi|$, and the effective Hamiltonian

$$H_{\text{eff}} = -i \sum_{i=1}^m \left(\frac{\eta'_A}{2} a_{A_i}^\dagger a_{A_i} + \frac{\eta'_B}{2} a_{B_i}^\dagger a_{B_i} \right). \quad (26)$$

In Eqs. (25) and (26), we assumed that the total loss rates η'_A and η'_B are the same for the m entangled pairs, but η'_A and η'_B may be different from each other. In this section, we will show how to distill entanglement from the kind of realistic continuous entangled states described by the solution of the master equation (25). There are two practical circumstances in which our entanglement purification protocol can be extended straightforwardly to generate maximally entangled states from the mixed Gaussian entangled states. We describe these two circumstances one by one.

A. Case of small state preparation noise

Though the state preparation noise is unavoidable, in many cases it is reasonable to assume that it is quite small. We take $\eta'_A \tau$ and $\eta'_B \tau$ as small factors, and solve the master equation (25) perturbatively to the first order of these small factors. It is convenient to use the quantum trajectory language to explain the perturbative solution.

In this language, to the first order of $\eta'_A\tau$ and $\eta'_B\tau$, the final normalized state of the m entangled pairs is either (no jumps)

$$\begin{aligned} |\Psi^{(0)}\rangle_{(A_i B_i)} &= \frac{1}{\sqrt{p^{(0)}}} e^{-iH_{\text{eff}}\tau} |\Psi\rangle_{(A_i B_i)} \\ &= \frac{1}{\sqrt{p^{(0)}}} (1 - \lambda^2)^{\frac{m}{2}} \sum_{j=0}^{\infty} \lambda^j e^{-\frac{\eta'_A + \eta'_B}{2}\tau j} \sqrt{f_j^{(m)}} |j\rangle_{(A_i B_i)} \end{aligned}$$

with probability

$$p^{(0)} = \frac{(1 - \lambda^2)^m}{(1 - \lambda^2 e^{-(\eta'_A + \eta'_B)\tau})^m} \quad (28)$$

or (a jump occurred)

$$|\Psi^{(\alpha_i)}\rangle_{(A_i B_i)} = \frac{1}{\sqrt{p^{(\alpha_i)}}} \sqrt{\eta'_{\alpha}\tau} a_{\alpha_i} |\Psi\rangle_{(A_i B_i)}, \quad (\alpha = A, B \text{ and } i = 1, 2, \dots, m) \quad (29)$$

with probability

$$\begin{aligned} p^{(\alpha_i)} &= \eta'_{\alpha}\tau \langle \Psi | a_{\alpha_i}^\dagger a_{\alpha_i} | \Psi \rangle_{(A_i B_i)} \\ &= \bar{n} \eta'_{\alpha}\tau, \end{aligned} \quad (30)$$

where $\bar{n} = \langle \Psi | a_{\alpha_i}^\dagger a_{\alpha_i} | \Psi \rangle_{(A_i B_i)} = \sinh^2(r)$ is the mean photon number for a single mode.

Similar to the pure state case, we also use QND measurements of the total photon number to distill entanglement from the mixed continuous state described by Eqs. (27)-(30). The difference is that now we perform QND measurements on both sides A and B. The measurement results are denoted by j_A and j_B , respectively. We then compare j_A and j_B through classical communication, and keep the outcome state if and only if $j_A = j_B$. It is easy to show that the final state is a maximally entangled state in a finite dimensional Hilbert space. Let $P_A^{(j)}$ and $P_B^{(j)}$ denote the projections onto the eigenspace of the corresponding total number operator $\sum_{i=1}^m a_{A_i}^\dagger a_{A_i}$ and $\sum_{i=1}^m a_{B_i}^\dagger a_{B_i}$ with eigenvalue j , respectively. From Eqs. (27) and (29), it follows

$$\begin{aligned} P_A^{(j)} P_B^{(j)} |\Psi^{(0)}\rangle_{(A_i B_i)} &= |j\rangle_{(A_i B_i)}, \\ P_A^{(j)} P_B^{(j)} |\Psi^{(\alpha_i)}\rangle_{(A_i B_i)} &= 0, \quad (\alpha = A, B \text{ and } i = 1, 2, \dots, m) \end{aligned}$$

So if $j_A = j_B$, the outcome state is maximally entangled with entanglement $\log(f_j^{(m)})$. The components (29) in the mixed density operator, which are not maximally entangled, are discarded through confirmation of the two-side measurement outcomes. Compared with the pure state case, the probability to get the entangled state $|j\rangle_{(A_i B_i)}$ is now decreased to

$$p'_j = (1 - \lambda^2)^m \lambda^{2j} f_j^{(m)} e^{-(\eta'_A + \eta'_B)\tau j}. \quad (32)$$

We also note that the projection operators $P_A^{(j)} P_B^{(j)}$ cannot eliminate the state obtained from the initial state $|\Psi\rangle_{(A_i B_i)}$ by a quantum jump on both sides A and B. The total probability for this kind of quantum jumps to occur is proportional to $m^2 \bar{n}^2 \eta'_A \eta'_B \tau^2$. So the condition for a small state preparation noise in fact requires

$$m^2 \bar{n}^2 (\eta_A \tau + \eta_0 / \kappa_c) (\eta_B \tau + \eta_0 / \kappa_c) \ll 1. \quad (33)$$

If the light transmission loss is the dominant noise, Eq. (33) reduces to $m^2 \bar{n}^2 \eta_A \eta_B \tau^2 \ll 1$.

B. Case of asymmetric state preparation noise

In the above purification protocol, we need classical communication (CC) to confirm that the measurement outcomes of the two sides are the same, and during this CC, we implicitly assume that the storage noise for the cavity modes is negligible. In fact, that the storage noise during CC is much smaller than the transmission noise is a common assumption made in all the entanglement purification schemes which need the help of repeated CCs [3,5]. If we also make this assumption for continuous variable systems, there exists a simple purification protocol to generate maximally entangled states. We put the NOPA setup on the A side. After creation of ideal squeezed vacuum lights, we directly couple one output light of the NOPA to the cavity on side A without noisy propagation; and the other output of the NOPA is sent to the remote side B, through a long distance noisy transmission. This configuration of the setup is equivalent to setting the transmission loss rate $\eta_A \approx 0$ so that $\eta'_A \approx \eta_0 / (\kappa_c \tau)$. Note that the NOPA cavity loss rate η_0 is normally much smaller than the output coupling rate κ_c , so the total loss rate η'_A can be much smaller than η'_B in this case. The purification protocol now is exactly the same as that described in the previous case. We note that the component of the mixed density operator which is kept the projection $P_A^{(j)} P_B^{(j)}$ should subject to the same times of quantum jumps on each side A and B. We want this component is a maximally entangled state. This requires that the total probability for A and B to be subjected to the same nonzero number of quantum jumps should be very small. From Eq. (30), this total probability is always smaller than $m \bar{n} \eta'_A \tau$, no matter how large the transmission loss $\eta_B \tau$ is. So the working condition of the protocol in the asymmetric transmission noise case is

$$m \bar{n} \eta_0 / \kappa_c \ll 1. \quad (34)$$

The transmission loss $\eta_B \tau$ can be above one. The probability of success for obtaining the maximally entangled state $|j\rangle_{(A_i B_i)}$ is also given by Eq. (32).

Before concluding this section, we remark that for continuous variable systems, the information carrier is normally light, and the assumption of storage with a very small loss rate is typically unrealistic. It is interesting to note that recently there have been proposals to store light in internal states of an atomic ensemble [21,22]. If this turns out to be possible, the storage time for light can be greatly increased. Anyway, as was pointed out in [14], this purification method is in fact not essentially hampered by the difficulty to store light, since there is a simple posterior confirmation method to circumvent the storage problem. Note that the purpose to distill maximally entangled states is to directly apply them in some quantum communication protocol, such as in quantum cryptography or in quantum teleportation. So we can modify the above purification protocol by the following procedure: right after the cavity A attains its steady state, we make a QND measurement of the total excitation number on side A and get a measurement result j_A . Then we do not store the outcome state on side A, but immediately use it (e.g., perform the corresponding measurement as required by a quantum cryptography protocol). During this process, the modes B_i are being sent to the distant side B, and when they arrive, we make another QND measurement of the total excitation number of the modes B_i and get a outcome j_B . The resulting state on side B can be directly used (for quantum cryptography for instance) if $j_A = j_B$, and discarded otherwise. By this method, we formally get maximally entangled states through posterior confirmation, and at the same time we need not store the modes on both sides.

V. QND MEASUREMENTS OF THE TOTAL PHOTON NUMBER OF SEVERAL CAVITIES

The QND measurement of the total photon number plays a critical role in our entanglement purification protocol. There have been some proposals for making a QND measurement of the photon number in a single cavity [23–25], such as letting some atoms pass through the cavity, and measuring the internal or external degrees of freedom of the atoms [23]. In this section, we propose a purely optical scheme for making a QND measurement of the total photon number contained in several cavities. The different optical modes interact with each other through cross phase modulation induced by a Kerr medium, and we use cavities to enhance this kind of interaction. As an illustrative example, in the following we will show how to measure the total photon number of two cavities. Extension of this scheme to include several cavities is straightforward.

The schematic setup is depicted in Fig. 5. We want to make a QND measurement of the total photon number $n_1 + n_2$ contained in the good cavities I and II, whose damping rate κ is assumed to be very small. The cavities I and II, each with a Kerr type medium inside, are put respectively in a bigger ring cavity. The two ring

cavities are assumed to damp at the same rate γ , and $\gamma \gg \kappa$. A strong coherent light b_{i1} is incident on the first ring cavity, whose output b_{o1} is directed to the second ring cavity. The output b_{o2} of the second ring cavity is continuously observed through homodyne detection, and we will show that under some realistic conditions, this detection gives a QND measurement of the total photon number operator $n_1 + n_2 = a_1^\dagger a_1 + a_2^\dagger a_2$.

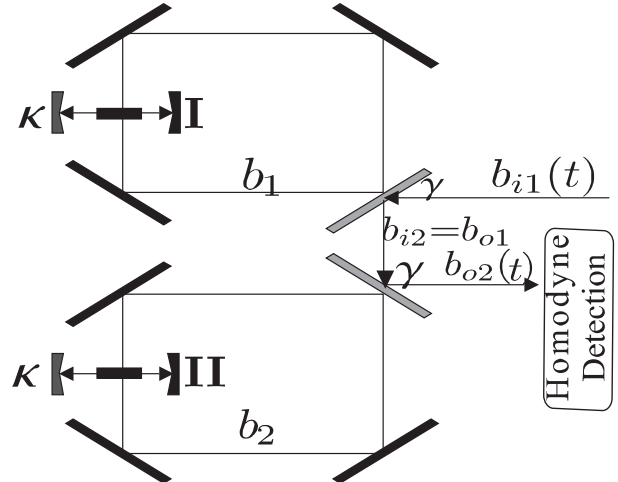


FIG. 5. Schematic experimental setup to measure the total photon number $n_1 + n_2$ contained in the cavities I and II.

The measurement model depicted in Fig. 5 is an example of a cascaded quantum system [18]. The incident light b_{i1} can be expressed as

$$b_{i1} = b'_{i1} + g\sqrt{\gamma}, \quad (35)$$

where $g\sqrt{\gamma}$ is a constant driving field, and b'_{i1} is the standard vacuum white noise, satisfying

$$\begin{aligned} \langle b'_{i1}{}^\dagger(t) b'_{i1}(t') \rangle &= 0, \\ \langle b'_{i1}(t) b'_{i1}{}^\dagger(t') \rangle &= \delta(t - t'). \end{aligned} \quad (36)$$

The Hamiltonian for the Kerr medium is assumed to be

$$H_i = \hbar\chi n_i b_i^\dagger b_i, \quad (i = 1, 2), \quad (37)$$

where b_1 and b_2 are the annihilation operators for the ring cavity modes, and χ is the cross-phase modulation coefficient. The self-phase modulation effects will be discussed in the next section and shown to be negligible under some realistic conditions. In the rotating frame, the Langevin equations describing the dynamics in the two ring cavities have the form

$$\begin{aligned} \dot{b}_1 &= -i\chi n_1 b_1 - \frac{\gamma}{2} b_1 - \sqrt{\gamma} b'_{i1} - g\gamma, \\ \dot{b}_2 &= -i\chi n_2 b_2 - \frac{\gamma}{2} b_2 - \sqrt{\gamma} b_{o1} \end{aligned} \quad (38)$$

The boundary conditions for the two ring cavities are described by

$$\begin{aligned} b_{i2} &= b_{o1} = b'_{i1} + g\sqrt{\gamma} + \sqrt{\gamma}b_1, \\ b_{o2} &= b_{i2} + \sqrt{\gamma}b_2. \end{aligned} \quad (39)$$

Assume $\gamma \gg \chi \langle n_i \rangle$, ($i = 1, 2$), and we take adiabatic elimination, i.e., let $\dot{b}_1 = \dot{b}_2 = 0$ in Eq. (38), obtaining

$$\begin{aligned} b_1 &\approx \frac{-2(g\gamma + \sqrt{\gamma}b'_{i1})}{\gamma} \left(1 - \frac{2i\chi n_1}{\gamma}\right), \\ b_2 &\approx \frac{2(g\gamma + \sqrt{\gamma}b'_{i1})}{\gamma} \left(1 - \frac{4i\chi n_1}{\gamma} - \frac{2i\chi n_2}{\gamma}\right) \end{aligned} \quad (40)$$

Substituting the above result into Eq. (39), the final output field b_{o2} is expressed as

$$b_{o2} \approx -\frac{4ig\chi}{\sqrt{\gamma}}(n_1 + n_2) + b'_{i1} + g\sqrt{\gamma}. \quad (41)$$

Now we measure the X -component of the quadrature phase amplitudes of the output field b_{o2} through a homodyne detection. The phase of the driving field g is set according to $g = i|g|$. Suppose T is the measuring time. What we really get is the integrated photon current over time T , which, divided by T , corresponds to the following measuring operator

$$\begin{aligned} X_T &= \frac{1}{T} \int_0^T \frac{1}{\sqrt{2}} [b_{o2}(t) + b_{o2}^\dagger(t)] dt \\ &\approx \frac{4\sqrt{2}|g|\chi}{\sqrt{\gamma}}(n_1 + n_2) + \frac{1}{\sqrt{T}} X_T^{(b)}, \end{aligned} \quad (42)$$

where $X_T^{(b)} = \frac{1}{\sqrt{2}}(b_T + b_T^\dagger)$, and b_T , satisfying $[b_T, b_T^\dagger] = 1$, is defined by

$$b_T = \frac{1}{\sqrt{T}} \int_0^T b'_{i1}(t) dt. \quad (43)$$

From Eq. (36), it follows that the defined mode b_T is in a vacuum state. So the first term of the right hand side of Eq. (42) represents the signal which is proportional to $n_1 + n_2$, and the second term represents the contribution of the vacuum noise. The distinguishability of this measurement is given by

$$\delta n = \frac{\sqrt{\gamma}}{8|g|\chi\sqrt{T}}. \quad (44)$$

If $\delta n < 1$, i.e., if the measuring time

$$T > \frac{\gamma}{64|g|^2\chi^2}, \quad (45)$$

we perform an effective measurement of the total number operator $n_1 + n_2$. During the measuring time T , the loss of the two cavities I and II should be negligible, which requires

$$\kappa \langle n_i \rangle T < 1, \quad (i = 1, 2) \quad (46)$$

Under this condition, $n_1 + n_2$ is approximately a conserved observable, and we realize a QND measurement of the total photon number operator. The measurement projects the field in the cavities I and II to one of the eigenstates of $n_1 + n_2$. Eqs. (45) and (46), combined together, determine the suitable choice for the measuring time.

VI. INFLUENCE OF IMPERFECTIONS IN THE QND MEASUREMENT

We have shown how to perform a QND measurement of the total photon number. The scheme described above works under ideal conditions. For a real experiment, there are always many imperfections which should be considered. For example, the phase of the driving field may be unstable, and has a small variance; the damping rates and the cross phase modulation coefficients for different ring cavities may not be exactly the same; the Kerr media and the mirrors may absorb some light; self-phase modulation effects caused by the Kerr media may have some influence on the resulting state; there may be some loss of light from the first ring cavity to the second ring cavity; the efficiency of the detector is not unity. Of course, to realize a QND measurement of the total photon number, all the imperfections must be small. But the important question is how small these imperfections should be. In this section, we will deduce quantitative requirements for all the imperfections listed above. These calculations may be helpful for a future real experiment. We will consider these imperfections one by one.

A. Phase instability of the driving field

Assume that the phase of the driving field $g\sqrt{\gamma}$ has a small variance δ , i.e., g is expressed as $g = i|g|e^{i\delta}$. Then, Eq. (42) is replaced by

$$X_T \approx \frac{4\sqrt{2}|g|\chi}{\sqrt{\gamma}}(n_1 + n_2) + \frac{1}{\sqrt{T}} X_T^{(b)} - \sqrt{2}|g|\delta\sqrt{\gamma}, \quad (47)$$

The last term of Eq. (47) represents the noise due to the phase instability of the driving field. It should be negligible compared with the signal, which requires

$$\delta < \frac{4\chi}{\gamma}. \quad (48)$$

On the other hand, we know that the squared phase variance δ^2 increases linearly with time, i.e. $\delta^2 = \delta_t t$, where δ_t is the increasing rate. The measuring time T is bounded from below by Eq. (45), so the increasing rate of the phase instability of the driving field is required to satisfy

$$\delta_t < \frac{1024|g|^2\chi^4}{\gamma^3}. \quad (49)$$

Eq. (49) suggests it is easier to meet the requirement imposed by the phase instability with a strong driving field and a large cross phase modulation coefficient.

B. Imbalance between the ring cavities

In the previous section, we assumed that the damping rates and the cross phase modulation coefficients are exactly the same for the two ring cavities. This may be impossible in a real experiment. Here we calculate the largest allowed imbalance between the two ring cavities. The damping rates and the cross phase modulation coefficients for the ring cavities are denoted by γ_1, γ_2 and χ_1, χ_2 , respectively. The Langevin equations (38) and the boundary conditions (39) are replaced respectively by the following equations

$$\begin{aligned} \dot{b}_1 &= -i\chi_1 n_1 b_1 - \frac{\gamma_1}{2} b_1 - \sqrt{\gamma_1} b'_{i1} - g\gamma_1, \\ \dot{b}_2 &= -i\chi_2 n_2 b_2 - \frac{\gamma_2}{2} b_2 - \sqrt{\gamma_2} b_{i2} \end{aligned} \quad (50)$$

$$\begin{aligned} b_{i2} &= b_{o1} = b'_{i1} + g\sqrt{\gamma_1} + \sqrt{\gamma_1} b_1, \\ b_{o2} &= b_{i2} + \sqrt{\gamma_2} b_2. \end{aligned} \quad (51)$$

The final measured observable is expressed as

$$X_T \approx \frac{4\sqrt{2}|g|\chi_1}{\sqrt{\gamma_1}} (n_1 + n_2) + \frac{1}{\sqrt{T}} X_T^{(b)} + 4\sqrt{2}|g|\sqrt{\gamma_1} \left(\frac{\chi_2}{\gamma_2} - \frac{\chi_1}{\gamma_1} \right) n_2, \quad |\beta_2^2 - \beta_1^2| < \frac{\gamma^2}{\langle n_2 \rangle}. \quad (52)$$

The last term of Eq. (52) represents the noise due to the unbalance between the ring cavities, which should be negligible compared with the signal, yielding

$$\left| \frac{\chi_2 \gamma_1}{\chi_1 \gamma_2} - 1 \right| < \frac{1}{\langle n_2 \rangle}. \quad (53)$$

C. Absorption and leakage of the light

Light absorption by mirrors and Kerr media and light leakage through other mirrors of the ring cavities can be described by the same Langevin equation, which has the form

$$\begin{aligned} \dot{b}_1 &= -i\chi n_1 b_1 - \frac{\gamma}{2} b_1 - \sqrt{\gamma} b'_{i1} - g\gamma - \frac{\beta_1}{2} b_1 - \sqrt{\beta_1} c_{i1}, \\ \dot{b}_2 &= -i\chi n_2 b_2 - \frac{\gamma}{2} b_2 - \sqrt{\gamma} b_{i2} - \frac{\beta_2}{2} b_2 - \sqrt{\beta_2} c_{i2}, \end{aligned} \quad (54)$$

where β_1 and β_2 are the light leakage (or absorption) rates of the first and second ring cavities, respectively,

and c_{i1} and c_{i2} are the standard vacuum inputs. The boundary conditions for the ring cavities are still described by Eq. (39). The leaked (or absorbed) light fields c_{o1} and c_{o2} are expressed as

$$c_{o\alpha} = c_{i\alpha} + \sqrt{\beta_\alpha} b_\alpha, \quad (\alpha = 1, 2). \quad (55)$$

The leakage (or absorption) of light may have two types of effects: First, it may destroy the balance between the two ring cavities; and second, the leaked light (55) may carry some information about n_1 (or n_2). Any information about n_1 (or n_2) will destroy the superposition of the different eigenstates of n_1 (or n_2), and thus lead to decoherence of the eigenstate of $n_1 + n_2$ (Note that an eigenstate of $n_1 + n_2$ is normally a superposition of the different eigenstates of n_1 (or n_2)). So we require that the information about n_1 (or n_2) carried by the leaked light should be completely masked by the vacuum noise. This is equivalent to require that the decoherence of the eigenstate of $n_1 + n_2$ caused by the light leakage is negligible. To consider the first effect of the light leakage, we calculate the measured observable X_T , and find it has the form

$$X_T \approx \frac{4\sqrt{2}|g|\chi}{\sqrt{\gamma}} (n_1 + n_2) + \frac{1}{\sqrt{T}} X_T^{(b)} + \frac{4\sqrt{2}|g|\chi}{\sqrt{\gamma}} \left(\frac{\beta_2^2}{\gamma^2} - \frac{\beta_1^2}{\gamma^2} \right) n_2, \quad (56)$$

The last term of Eq. (56) should be negligible compared with the signal, which requires

$$|\beta_2^2 - \beta_1^2| < \frac{\gamma^2}{\langle n_2 \rangle}. \quad (57)$$

To consider the decoherence effect of the light leakage, we define a similar measuring operator $X_T^{(\alpha)}$ for the leaked light (55)

$$\begin{aligned} X_T^{(\alpha)} &= \frac{1}{T} \int_0^T \frac{1}{\sqrt{2}} [c_{o\alpha}(t) + c_{o\alpha}^\dagger(t)] dt \\ &\approx \frac{8\sqrt{2}|g|\chi\sqrt{\beta_\alpha}(\alpha-1)}{\gamma} (n_1 + n_2) + \frac{1}{\sqrt{T}} X_T^{(c_\alpha)} \\ &\quad - \frac{4\sqrt{2}|g|\chi\sqrt{\beta_\alpha}}{\gamma} n_\alpha, \quad (\alpha = 1, 2), \end{aligned} \quad (58)$$

where $X_T^{(c_\alpha)}$, similar to $X_T^{(b)}$ defined below Eq. (42), are standard vacuum noise terms. The last term of Eq. (58) bears some information about n_α , which should be completely masked by the vacuum noise term to make the decoherence effect negligible. This condition requires

$$\frac{4\sqrt{2}|g|\chi\langle n_\alpha \rangle}{\gamma} \sqrt{\beta_\alpha} < \frac{1}{\sqrt{2T}}. \quad (59)$$

On the other hand, the measuring time T is bounded from below by Eq. (45), which, combined with Eq. (59), yields the following requirement for the leakage rates

$$\beta_\alpha < \frac{\gamma}{\langle n_\alpha \rangle^2}, \quad (\alpha = 1, 2). \quad (60)$$

Obviously, this is a much stronger requirement than that given by Eq. (57).

We should mention that there is another kind of absorption by the Kerr medium, the absorption rate of which is proportional to the cavity photon number n_α . This kind of absorption, usually termed two-photon absorption, cannot be described by Eq. (54). To incorporate the two-photon absorption, we add an imaginary part to the cross phase modulation coefficient χ , i.e., χ is replaced by $\chi + i\chi_i$, where χ_i describes the two-photon absorption rate. The two-photon absorption should be negligible compared with the cross Kerr interaction, which requires $\chi_i < \frac{\chi}{\langle n_\alpha \rangle}$, ($\alpha = 1, 2$).

D. Self-phase modulation effects

Normally, a Kerr medium also induces self-phase modulation effects. However, by a suitable choice of the resonance condition for the Kerr medium, the self-phase modulation effects can be made much smaller than the cross-phase modulation [26], then the self phase modulation interaction is basically negligible. Here, for completeness, we still calculate the influence of self-phase modulations. In fact, self-phase modulation of the ring cavity modes have no influence on the QND measurement. This modulation adds a term like $-i\chi_s b_i^\dagger b_i b_i$ ($i = 1, 2$) in the Langevin equation (38), where χ_s denotes the self-phase modulation coefficient for the ring cavity modes. We know that the ring cavity modes b_1 and b_2 are in steady states under adiabatic elimination, and to a good approximation $b_i^\dagger b_i$ can be replaced by $\langle b_i^\dagger b_i \rangle = 4|g|^2$.

So the term $-i\chi_s b_i^\dagger b_i b_i$ simply induces a constant phase shift for the output field b_{o2} , and it can be easily compensated by choosing the initial phase of the driving field g .

Self phase modulation of the cavity modes a_1 and a_2 plays a more subtle role. First, it obviously has no influence on the QND measurement of $n_1 + n_2$, but it influences the resulting state after the QND measurement. In the purification scheme for two entangled pairs (described in section III.A), if there is no self-phase modulation, the state after the QND measurement is given by Eq. (13); and if the self-phase modulation of the modes a_1 and a_2 is considered, the modulation Hamiltonian $\hbar\chi'_s n_i^2$ ($i = 1, 2$), in which χ'_s is the corresponding self phase modulation coefficient, will bring the resulting state into

$$|j\rangle'_{A_1 A_2 B_1 B_2} = \frac{1}{\sqrt{1+j}} \sum_{n=0}^j e^{i\chi'_s t [n^2 + (j-n)^2]} |n, j-n\rangle_{A_1 A_2} |n, j-n\rangle_{B_1 B_2}, \quad (61)$$

where t is the interaction time for the self phase modulation. It is important to note that the state (61) is still a maximally entangled state with entanglement $\log(j+1)$. In this sense, self-phase modulation effects have no influence on the entanglement purification, though the resulting state is changed.

E. Imperfect coupling from the first ring cavity to the second ring cavity

If the coupling between the two ring cavities is not perfect, the relation $b_{i2} = b_{o1}$ is not valid any more, and should be replaced by

$$\begin{aligned} b_{i2} &= \sqrt{\mu} b_{o1} + \sqrt{1-\mu} d_i, \\ d_o &= \sqrt{\mu} d_i + \sqrt{1-\mu} b_{o1}, \end{aligned} \quad (62)$$

where d_i is the standard vacuum white noise, and d_o represents the leaked light in the imperfect coupling. The quantity μ describes the coupling efficiency. This kind of imperfection is very similar to the light leakage (or absorption) described in subsection VI.C. The difference is that the imperfect coupling (62) does not cause any unbalance between the two ring cavities. The only restriction is that the decoherence effect induced by it should be negligible, which requires

$$\mu > 1 - \frac{1}{\langle n_1 \rangle^2}. \quad (63)$$

Eq. (63) suggests that loss of light from the first to the second ring cavity should be very small.

F. Detector inefficiency

The detector efficiency of course cannot attain 1. For a detector with efficiency ν , the real measured field b'_{o2} has the following relation with the output of the second ring cavity

$$b'_{o2} = \sqrt{\nu} b_{o2} + \sqrt{1-\nu} e_i, \quad (64)$$

where e_i is the standard vacuum white noise. This imperfection is similar to the imperfect coupling considered in the previous subsection. But now the leaked light depends only on the operator sum $n_1 + n_2$, and carries no information about the single cavity photon number n_1 , so it does not induce any decoherence. The only role played by the detector inefficiency is that it decreases the signal by a factor $\sqrt{\nu}$, so Eq. (45) on the restriction of the measuring time is now replaced by

$$T > \frac{\gamma}{64\nu |g|^2 \chi^2}, \quad (65)$$

Obviously, the detector inefficiency has no important influence on this QND measurement scheme.

VII. SUMMARY AND DISCUSSION

In summary, we have given a detailed description of the purification protocol which generates maximally entangled states in a finite dimensional Hilbert space from two-mode squeezed states or from realistic Gaussian continuous entangled states. The nonlocal Gaussian continuous entangled states are generated by feeding two distant cavities with the outputs of the NOPA. The purification operation is based on a local QND measurement of the total photon number contained in several cavities. We have extensively analyzed a cavity scheme to do this QND measurement, and have deduced its working condition. Furthermore, we have discussed many imperfections existing in a real experiment, and deduced quantitative requirements for the relevant experimental parameters. In Tab. 1, we summarize the working conditions for the collective QND measurement, including the requirements for many types of imperfections.

Measuring time	$\frac{\gamma}{64 g ^2\chi^2} < T < \frac{1}{\kappa\langle n_i \rangle}$
Phase instability	$\delta < \frac{4\chi}{\gamma}$ or $\delta_t < \frac{1024 g ^2\chi^4}{\gamma^3}$
Cavity imbalance	$\left \frac{\chi_2\gamma_1}{\chi_1\gamma_2} - 1 \right < \frac{1}{\langle n_2 \rangle}$
Absorption (leakage) rate	$\beta_\alpha < \frac{\gamma}{\langle n_\alpha \rangle^2}, (\alpha = 1, 2)$
Coupling efficiency	$\mu > 1 - \frac{1}{\langle n_1 \rangle^2}$
Detector efficiency	$\nu > \frac{\gamma}{64 g ^2\chi^2T}$

TABLE I. List of requirements for the QND measurement

To realize the QND measurement, basically we need high finesse optical cavities and strong cross Kerr interaction media. A good example for the strong cross Kerr interaction is provided by the resonantly enhanced Kerr nonlinearity, which has been predicted theoretically [26,27] and demonstrated in recent experiments [28]. In those works, the Kerr medium is a low density cold trapped atomic gas, whose relevant energy level structure is represented by the four-state diagram shown in Fig. 6 with $|1\rangle$ being the ground state. The ring cavity mode b_i with frequency ω_b is assumed to be resonant with the $|1\rangle \rightarrow |3\rangle$ transition, and the cavity mode a_i with frequency ω_a (ω_a is quite different from ω_b) is coupled to the $|2\rangle \rightarrow |4\rangle$ transition, but with a large detuning Δ_{42} . A nonperturbative classical coupling field with frequency ω_c resonant with the $|2\rangle \rightarrow |3\rangle$ transition creates an electromagnetically induced transparency (EIT) for the cavity fields a_i and b_i .

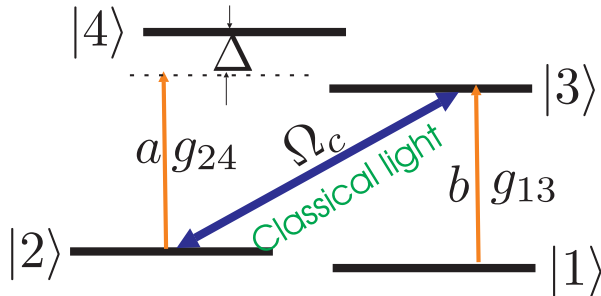


FIG. 6. Level structure of the atoms.

In this configuration, the one-photon absorption of the medium is eliminated due to quantum interference, and the cross Kerr nonlinearity is only limited by the two-photon absorption (the self Kerr nonlinearity is negligible provided that $|\omega_a - \omega_b| \gg \Delta_{42}$). After adiabatically eliminating all the atomic levels, the cross phase modulation coefficient is given by [26]

$$\chi \sim \frac{3|g_{13}|^2|g_{24}|^2}{\Omega_c^2 \Delta_{42}} n_{\text{atom}}, \quad (66)$$

where g_{24} and g_{13} are the coupling coefficients between the atoms and the cavity modes a_i and b_i , respectively, Ω_c denotes the Rabi frequency of the coupling field, and n_{atom} is the total atom number contained in the cavity. The two-photon absorption rate χ_i is connected with χ by the relation $\chi_i/\chi = \gamma_{42}/\Delta_{42}$, where $2\gamma_{42}$ is the spontaneous emission rate from level $|4\rangle$ to level $|2\rangle$. To justify the adiabatic elimination, one requires that $\frac{|g_{13}|^2 n_{\text{atom}}}{\Omega_c^2} < 1$ [29,30]. As an estimation, if one takes $\frac{|g_{13}|^2 n_{\text{atom}}}{\Omega_c^2} \sim 0.2$, $g_{24}/2\pi \sim 10\text{MHz}$, $\gamma_{42}/2\pi \sim 30\text{MHz}$, and $\Delta_{42} \sim 10\gamma_{42}$, the coefficient χ is about $\chi/2\pi \sim 0.2\text{MHz}$, and the two-photon absorption rate $\chi_i \sim 0.1\chi$. This value of the cross phase modulation coefficient χ is not large enough to realize a single-photon turnstile device [26], but it is

enough for performing QND measurements of the photon number. For example, if the mean photon number $\langle n_1 \rangle = \langle n_2 \rangle = \sinh^2(r) \sim 1.4$ with the squeezing parameter $r \sim 1.0$, we choose the decay rates $\kappa/2\pi \sim 4\text{MHz}$ and $\gamma/2\pi \sim 100\text{MHz}$ (these values for decay rates are obtainable in current experiments), and let $g \sim 50$ (for a cavity with cross area $S \sim 0.5 \times 10^{-4}\text{cm}^2$, $g \sim 50$ corresponds to a coherent driving light with intensity about 10mWcm^{-2}). With the above parameters, all the requirements listed in Tab. 1 can be satisfied if we choose the measuring time $T \sim 8\text{ns}$. Note that the light speed can be much reduced in the EIT medium [28], so it is possible to get a reduced cavity decay rate κ with the same finesse mirrors, and then more favorable parameters can be given for the QND measurement. Note also that a large Kerr nonlinearity based on EIT can also be obtained in other systems, such as trapping a single atom in a high finesse cavity [31]. So the example discussed here is not the unique choice.

We thank P. Grangier and S. Parkins for discussions. This work was supported by the Austrian Science Foundation, by the European TMR network Quantum Information, and by the Institute for Quantum Information. GG acknowledges support by the Friedrich-Naumann-Stiftung.

-
- [1] C. H. Bennett, Phys. Today 48 (10), 24 (1995)
 - [2] J. I. Cirac et al., Phys. Rev. Lett. 78, 3221 (1997); S. J. Enk, J. I. Cirac, and P. Zoller, Science 279, 205 (1998).
 - [3] C. H. Bennett et al., Phys. Rev. Lett. 76, 722 (1996).
 - [4] C. H. Bennett et al., Phys. Rev. A 53, 2046 (1996).
 - [5] C. H. Bennett et al., Phys. Rev. A 54, 3824 (1996).
 - [6] L. Vaidman, Phys. Rev. A 49, 1473 (1994).
 - [7] S. L. Braunstein and J. Kimble, Phys. Rev. Lett. 80, 869 (1998).
 - [8] S. Lloyd and S. L. Braunstein, Phys. Rev. Lett. 82, 1784 (1999).
 - [9] S. L. Braunstein, Nature 394, 47 (1998); S. Lloyd and J. J.-E. Slotine, Phys. Rev. Lett. 80, 4088 (1998).
 - [10] T. C. Ralph, Phys.Rev.A. 61, 010302(R) (2000).
 - [11] L. M. Duan et al., Phys. Rev. Lett. 84, 2722 (2000); R. Simon, quant-ph/9909044.
 - [12] P. Horodecki and M. Lewenstein, quant-ph/0001035.
 - [13] A. Furusawa, et al., Science 282, 706 (1998).
 - [14] L. M. Duan, G. Giedke, J. I. Cirac, and P. Zoller, Phys. Rev. Lett 84, 4002 (2000).
 - [15] S. Parker, S. Bose, and M. B. Plenio, e-print quant-ph/9906098.
 - [16] T. Opatrny, G. Kurizki, and D.-G., Welsch, e-print quant-ph/9907048.
 - [17] Z. Y. Ou, et al., Phys. Rev. Lett. 68, 3663 (1992); A. S. Parkins and H. J. Kimble, e-print quant-ph/9907049.
 - [18] C. W. Gardiner and P. Zoller, *Quantum Noise* (Springer-Verlag, Berlin, 1999).

- [19] H. M. Wiseman, Phys. Rev. Lett. 75, 4587 (1995).
- [20] S. M. Barnett and D. T. Pegg, Phys. Rev. Lett. 76, 4148 (1996).
- [21] A. E. Kozhekin, K. Molmer, and E. S. Polzik, quant-ph/9912014.
- [22] M. D. Lukin, S. F. Yelin, and M. Fleischhauer, to appear in Phys. Rev. Lett. 84 (2000); L. M. Duan, J. I. Cirac, and P. Zoller (unpublished).
- [23] D. F. Walls and G. J. Milburn, *Quantum Optics* (Springer-Verlag, Berlin, 1995).
- [24] G. M. D'Ariano et al., quant-ph/0001065.
- [25] G. Nogues, et al., Nature 400, 239 (1999).
- [26] A. Imamoglu et al., Phys. Rev. Lett. 79, 1467 (1997); 81, 2836 (1998).
- [27] Y. Yamamoto, Nature 390, 17 (1997).
- [28] L. V. Hau et al., Nature 397, 594 (1999).
- [29] P. Grangier, D. F. Walls, and K. M. Gheri, Phys. Rev. Lett. 81, 2833 (1998).
- [30] K. M. Gheri, W. Alge, and P. Grangier, Phys. Rev. A, R2673 (1999).
- [31] S. Rebic, S. M. Tan, A. S. Parkins, and D. F. Walls, Quantum Semiclass. Opt. 1, 490 (1999).